

3D-Angiograms from 4 MR-Projections: A Quantitative Analysis

Alexander Brunner¹, Lei Zheng¹, Alexander Zyl¹, Florian Maier¹, Wolfhard Semmler¹, Jürgen Hesser², and Michael Bock^{1,3}

¹Dept. of Medical Physics in Radiology, German Cancer Research Center (DKFZ), Heidelberg, Germany; ²Experimental Radiation Oncology, University Medical Center Mannheim, Heidelberg University, Mannheim, Germany; ³Department of Radiology - Medical Physics, University Hospital Freiburg, Freiburg, Germany

Introduction

In real-time applications such as intravascular interventions the acquisition of 3D-angiograms is challenging as both image acquisition and 3D reconstruction need to be performed in less than 1 s. In this work, we present a new acquisition and reconstruction concept for 3D-angiograms which combines a fast projection acquisition pulse sequence with a multi-plane reconstruction. The approach was evaluated on a vessel bifurcation phantom and quantitatively compared to a high resolution dataset of the phantom.

Materials and Methods

Fast projection pulse sequence. For data acquisition, a stereoscopic double echo sequence [1] is used with tilted phase encoding directions (view tilting) between the first and the second echo to acquire two thick slice projections (stereo pair) of an object. The pulse sequence was extended to acquire 4 equiangular projections of an object. Therefore, the slice was rotated by 90° and an increased tilting angle of 45° was used (Fig. 1) to be able to perform multi-plane reconstructions. The pulse sequence was implemented on a clinical 1.5 T MR system (MAGNETOM Symphony, Siemens, Erlangen, Germany).

Vessel phantom. The concept was evaluated on a vessel bifurcation phantom. The tubes of the phantom (inner diameter: 5 mm) were filled with a contrast agent solution (0.9% NaCl, Gd-DTPA/H₂O: 1/200, Magnevist, Bayer Schering Pharma, Berlin, Germany) and embedded in a physiologic saline solution. The following imaging parameters were used: TR/TE₁/TE₂ = 5.5/1.6/3.7 ms, $\alpha = 30^\circ$, matrix: 204×256, FOV: 210×210 mm², slice thickness: 70 mm, bandwidth: 610 Hz/px, Partial Fourier-factor: 5/8, GRAPPA-factor 2 with 35 reference lines, 2/3 view sharing and 75% asymmetric echo acquisition. For comparison, a high resolution 3D dataset of the phantom was acquired with a 3D FLASH sequence (0.2×0.2×0.4 mm³).

Multi-plane reconstruction algorithm. The projection images were first binarized by thresholding (Fig. 2B). The centerline was determined in each projection using a binary thinning filter (Fig. 2C), while the diameter of each skeleton point was estimated by the Danielsson distance map [2] of the binary mask. In the second step (biplane reconstruction), for each projection pair, the corresponding skeleton points were assigned to each other based on the epipolar geometry [3]. For each point correspondence, the location and diameter of 3D point candidates were computed. The results of biplane reconstruction were verified by projecting these candidates to all considered projections. If one of its projections is not in the binary mask, it is not considered any more. Finally, the remaining candidate points were connected using Kruskal's algorithm [4] to span the vascular tree structure based on Euclidean distance between the points. The algorithm was implemented on a PC with CPU Intel i7 870 (2.93 GHz) and 8 GB RAM using C++.

Validation analysis. Prior to comparison, a reference tree structure was created by the binarization and centerline extraction of the high resolution 3D dataset. For comparison, the mean centerline distances, the mean radii differences, the bifurcation point distance and the Hausdorff distance between the tree structures were calculated. The Dice similarity coefficient was calculated between the reconstructed tree structure after voxelization and the binary mask of the high resolution 3D dataset.

Results

The image acquisition time of the 4 projections amounted to 726 ms, and the multi-plane reconstruction was calculated within 2.18 s for this dataset. For visual comparison of the volume dataset resulting from the multi-plane reconstruction and the high resolution acquisition, centerlines and surface renderings are illustrated in Fig. 3. Table 1 lists the results of the quantitative validation analysis.

Discussion

In this work, a novel concept for real-time reconstructions of 3D-angiograms is presented, which requires only 4 projection images of an object. The projections were acquired rapidly by the double echo projection sequence with frame rates of 1.4 Hz which could be further increased by reducing the resolution in phase encoding direction. In the present prototype implementation the reconstruction algorithm could not provide real-time images, but the additional speed-up factor of 3-4 required can easily be achieved using a multi-threaded implementation on GPUs.

The quantitative validation analysis revealed minor deviations between the two centerlines and corresponding radii. The maximum distance between the centerlines was 4 mm (Hausdorff distance), which can be explained by small structures due to imperfect closing plugs in the high resolution dataset (Fig. 3B) whereas these structures were excluded by thresholding in the projection dataset. The distance of the bifurcation point between the two datasets might be further reduced by optimizing the skeletonization step (cf. Fig. 2A). Here, the additional two projections completed the biplane reconstruction leading to a high correlation between the reconstructed 3D vessel bifurcation phantom and the high resolution 3D dataset (Dice similarity coefficient). In future implementations, the number of projections could be dynamically adapted to the complexity of the vessel structure to minimize the acquisition time.

In conclusion, we demonstrated that 3D-angiograms can be rapidly reconstructed from dedicated real-time projection images to visualize vascular trees for intravascular interventions.

Acknowledgement

This work was supported by the German Research Foundation (Bo 3025/2-1).

References

- [1] Brunner A, et al., *Proc. ESMRMB* 2011; 122; [2] Danielsson PE, *Comput. Graph. Image. Process.* 1980; [3] Hartley R, et al., *Cambridge Univ. Press* 2003; [4] Kruskal JB, *Proc. Amer. Math. Soc.* 1956

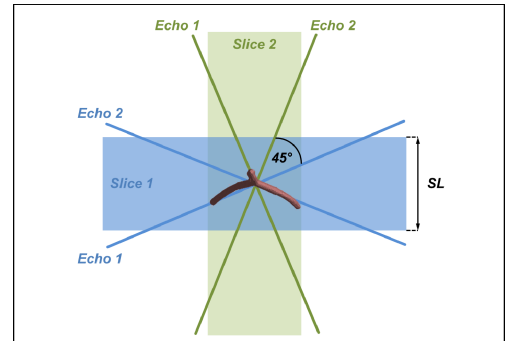


Fig. 1: Schematic of a targeted vessel bifurcation and the orientation of the 4 equiangular thick slice projections (green and blue lines). *Slice 1, echo 1* corresponds to 0°; *slice 1, echo 2* to 45° (blue); *slice 2, echo 1* to 90°; and *slice 2, echo 2* to 135° (green). *SL* denotes the slice thickness.

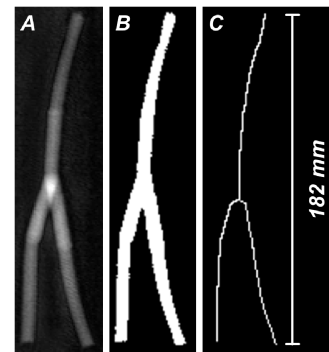


Fig. 2: Intermediate images of a selected projection of the vessel bifurcation phantom. A) measured projection image; B) binary image after thresholding; C) centerline of the binary image.

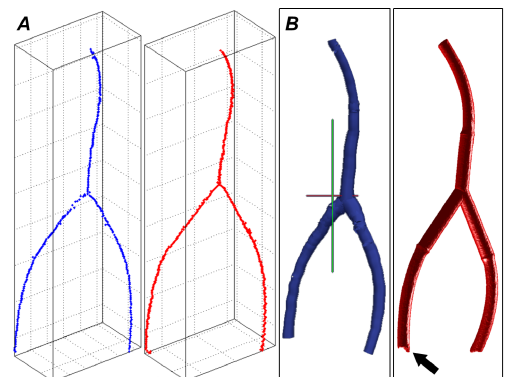


Fig. 3: Comparison between the multi-plane reconstruction (blue) and the 3D high resolution dataset (red). A) 3D centerlines; B) surface renderings. The arrow indicates a small structure caused by imperfect closing plugs.

Quality measure	Value \pm standard deviation
Mean centerline distances	1.0 \pm 0.5 mm
Mean radii differences	0.7 \pm 0.4 mm
Hausdorff distance	3.9 mm
Bifurcation point distance	2.2 mm
Dice similarity coefficient	0.72

Tab. 1: Results of the validation analysis.